

# Functional Characterization of *Corynebacterium alkanolyticum* $\beta$ -Xylosidase and Xyloside ABC Transporter in *Corynebacterium glutamicum*

Akira Watanabe,<sup>a</sup> Kazumi Hiraga,<sup>a</sup> Masako Suda,<sup>a</sup> Hideaki Yukawa,<sup>a</sup> Masayuki Inui<sup>a,b</sup>

Research Institute of Innovative Technology for the Earth, Kizugawa-shi, Kyoto, Japan<sup>a</sup>; Graduate School of Biological Sciences, Nara Institute of Science and Technology, Ikoma, Nara, Japan<sup>b</sup>

The *Corynebacterium alkanolyticum* *xylEFGD* gene cluster comprises the *xylD* gene that encodes an intracellular  $\beta$ -xylosidase next to the *xylEFG* operon encoding a substrate-binding protein and two membrane permease proteins of a xyloside ABC transporter. Cloning of the cluster revealed a recombinant  $\beta$ -xylosidase of moderately high activity (turnover for *p*-nitrophenyl- $\beta$ -D-xylopyranoside of  $111 \pm 4 \text{ s}^{-1}$ ), weak  $\alpha$ -L-arabinofuranosidase activity (turnover for *p*-nitrophenyl- $\alpha$ -L-arabinofuranoside of  $5 \pm 1 \text{ s}^{-1}$ ), and high tolerance to product inhibition ( $K_i$  for xylose of  $67.6 \pm 2.6 \text{ mM}$ ). Heterologous expression of the entire cluster under the control of the strong constitutive *tac* promoter in the *Corynebacterium glutamicum* xylose-fermenting strain X1 enabled the resultant strain X1EFGD to rapidly utilize not only xylooligosaccharides but also arabino-xylooligosaccharides. The ability to utilize arabino-xylooligosaccharides depended on *cgR\_2369*, a gene encoding a multitask ATP-binding protein. Heterologous expression of the contiguous *xylD* gene in strain X1 led to strain X1D with 10-fold greater  $\beta$ -xylosidase activity than strain X1EFGD, albeit with a total loss of arabino-xylooligosaccharide utilization ability and only half the ability to utilize xylooligosaccharides. The findings suggest some inherent ability of *C. glutamicum* to take up xylooligosaccharides, an ability that is enhanced by in the presence of a functional *xylEFG*-encoded xyloside ABC transporter. The finding that *xylEFG* imparts nonnative ability to take up arabino-xylooligosaccharides should be useful in constructing industrial strains with efficient fermentation of arabinoxylan, a major component of lignocellulosic biomass hydrolysates.

Hemicellulose, a heteropolymer of various pentose (D-xylose and L-arabinose) and hexose (D-glucose, D-mannose, and D-galactose) sugars, is a major component of plant cell walls (1). Its most common constituent is the polymer xylan, a linear backbone of  $\beta$ -1,4-linked D-xylose residues branched with various side groups such as acetyl, L-arabinofuranose, and O-methyl-D-glucuronic acid (2). Complete biological degradation of xylan necessitates removal of the side groups by accessory enzymes such as  $\alpha$ -L-arabinofuranosidases,  $\alpha$ -D-glucuronidase, and acetylxylan esterases for the linear backbone of D-xylose residues to be accessible to hydrolysis by endo- $\beta$ -1,4-xylanases and  $\beta$ -xylosidases (2). Xylanolytic microorganisms produce some or all of the enzymes necessary to utilize xylan as a carbon source. Fungal xylanolytic enzymes are usually secreted, whereas bacterial  $\alpha$ -L-arabinofuranosidases,  $\alpha$ -D-glucuronidase, and  $\beta$ -xylosidases are intracellular enzymes. In xylanolytic bacteria, extracellular xylooligosaccharides such as xylobiose and xylotriose resulting from the action of endo- $\beta$ -1,4-xylanases must be transported into the cells by carrier proteins prior to hydrolysis to xylose by intracellular  $\beta$ -xylosidases. Bacterial xylooligosaccharide transporters are either xyloside/ $\text{Na}^+$  ( $\text{H}^+$ ) symporters or xyloside ABC transporters. Xyloside/ $\text{Na}^+$  ( $\text{H}^+$ ) symporters are in essence multipass transmembrane proteins that transport xylooligosaccharides by sodium (proton) motive force. Xylooligosaccharide symporters able to transport as many as six (3) or as few as three (4) xylosyl units have been confirmed in *Klebsiella* spp. In contrast to symporter structure and mechanism, each xyloside ABC transporter is a complex of a substrate-binding protein, a membrane permease protein, and an ATP-binding protein that combine to facilitate the active transport of xylooligosaccharides across the cell membrane. To date, the only two confirmed xyloside ABC transporters are from

*Streptomyces thermoviolaceus* Bx1EFG (5) and *Geobacillus stearothermophilus* XynEFG (6). *S. thermoviolaceus* Bx1E and *G. stearothermophilus* XynE, the respective substrate-binding proteins of the transporters, have confirmed high affinities toward xylooligosaccharides, but their substrate specificities *in vivo* remain uncharacterized.

Corynebacteria are high-G+C-content Gram-positive actinomycetes that are widely distributed in nature in soil, water, and plants. Though no reported molecular characterization of xylanolytic enzymes and related transporters in corynebacteria is known, glutamate- and biosurfactant-producing *Corynebacterium alkanolyticum* (7, 8) grows on xylooligosaccharide as a sole carbon source. In this study, we clone  $\beta$ -xylosidase and xylooligosaccharide transporter genes from *C. alkanolyticum* and express them in the heterologous xylose-fermenting host *Corynebacterium glutamicum* (9). We consequently confirm the ability of the respective xylooligosaccharide transporter to transport both arabino-xylooligosaccharides and xylooligosaccharides. This is the first

Received 10 March 2015 Accepted 6 April 2015

Accepted manuscript posted online 10 April 2015

Citation Watanabe A, Hiraga K, Suda M, Yukawa H, Inui M. 2015. Functional characterization of *Corynebacterium alkanolyticum*  $\beta$ -xylosidase and xyloside ABC transporter in *Corynebacterium glutamicum*. Appl Environ Microbiol 81:4173–4183. doi:10.1128/AEM.00792-15.

Editor: M. Kivisaar

Address correspondence to Masayuki Inui, mmg-lab@rite.or.jp.

Copyright © 2015, American Society for Microbiology. All Rights Reserved.

doi:10.1128/AEM.00792-15

TABLE 1 Strains and plasmids used in this study

Strain or plasmid	Relevant characteristic(s)	Reference or source
<b>Strains</b>		
<i>E. coli</i>		
HS202	F' [ <i>traD36 proA</i> <sup>+</sup> <i>B</i> <sup>+</sup> <i>lacI</i> <sup>q</sup> <i>lacZ</i> ΔM15] D( <i>lac-proAB</i> ) <i>recA endA1 gyrA96 thi e14</i> mutant ( <i>mcrA</i> mutant), <i>supE44 relA1 ΔdeoR Δ(</i> <i>mrr-hsdRMS-mcrBC</i> )	TaKaRa
SCS110	<i>rpsL</i> (Str <sup>r</sup> ) <i>thr leu endA thi-1 lacY galK galT ara tonA tsx dam dcm supE44 Δ(lac-proAB)</i> [F' <i>traD36 proAB lacI</i> <sup>q</sup> ZΔM15]	Agilent
BL21(DE3)	F <sup>-</sup> <i>ompT hsdS<sub>B</sub>(r<sub>B</sub><sup>-</sup> m<sub>B</sub><sup>-</sup>) gal dcm</i> (DE3)	TaKaRa
<i>C. alkanolyticum</i> ATCC 21511		
<i>C. glutamicum</i>		
R	JCM18229	17
X1	Markerless <i>P<sub>trc</sub>-xylA</i> and <i>P<sub>trc</sub>-xylB</i> gene recombinant integrated into <i>XylI</i> of strain R	9
X1D	Km <sup>r</sup> ; <i>C. glutamicum</i> X1 bearing pCRF100	This work
X1EFGD	Km <sup>r</sup> ; <i>C. glutamicum</i> X1 bearing pCRF101	This work
X1(Δ2369)	<i>C. glutamicum</i> X1 Δ <i>cgR_2369</i>	This work
X1(Δ2369)D	Km <sup>r</sup> ; <i>C. glutamicum</i> X1Δ2369 bearing pCRF100	This work
X1(Δ2369)EFGD	Km <sup>r</sup> ; <i>C. glutamicum</i> X1Δ2369 bearing pCRF101	This work
X1(Δ2369)EFGDK	Km <sup>r</sup> ; <i>C. glutamicum</i> X1Δ2369 bearing pCRF102	This work
X1(Δ2369)EFGDM	Km <sup>r</sup> ; <i>C. glutamicum</i> X1Δ2369 bearing pCRF103	This work
BsrAXH	Km <sup>r</sup> ; <i>C. glutamicum</i> R bearing pCRF104	This work
<b>Plasmids</b>		
pCRB52T	Km <sup>r</sup> ; <i>P<sub>tac</sub></i> promoter; <i>E. coli-Corynebacterium</i> sp. shuttle vector derived from pHSG298 and pBY503	This work
pCRF100	Km <sup>r</sup> ; pCRB52T with a 2.4-kb NdeI-KpnI PCR fragment of the <i>xylD</i> gene	This work
pCRF101	Km <sup>r</sup> ; pCRB52T with a 5.6-kb NdeI-KpnI PCR fragment of the <i>xylEFGD</i> gene cluster	This work
pCRF102	Km <sup>r</sup> ; pCRF101 with a 1.1-kb KpnI PCR fragment of the <i>cgR_2369</i> gene	This work
pCRF103	Km <sup>r</sup> ; pCRF101 with a 1.1-kb KpnI PCR fragment of the <i>msiK</i> gene	This work
pCRF104	Km <sup>r</sup> ; pCRA725 with a 3.0-kb XbaI PCR fragment of the target sequence for deletion of the <i>cgR_2369</i> gene	This work
pCRA725	Km <sup>r</sup> ; pHSG298 with <i>P<sub>tac</sub>-sacR-sacB</i> genes	
pCRF105	Km <sup>r</sup> ; pCRB52T with a 1.5-kb NdeI-BglII PCR fragment of the <i>axh</i> gene	This work
pCRF106	Am <sup>r</sup> ; pColdII with a 2.4-kb NdeI-BglIII PCR fragment of the <i>xylD</i> gene	This work

confirmation of a bacterial arabino-xylooligosaccharide transporter, to the best of our knowledge. Given the efficacy of *C. glutamicum* to produce a variety of chemicals, including succinate (10), ethanol (11), isobutanol (12), alanine (13, 14), and valine (15), this study could contribute to better understanding and optimization of utilization of the arabinoxylan component of lignocellulosic biomass by *C. glutamicum* and further enhance the utility of the microorganism in the production of more valuable products from lignocellulosic biomass.

## MATERIALS AND METHODS

**Bacterial strains, medium, and cultivation conditions.** All bacterial strains and plasmids used in this study are listed in Table 1. For genetic manipulations, *Escherichia coli* strains were grown at 33°C in Luria-Bertani medium (16). For aerobic growth conditions, *C. alkanolyticum* and *C. glutamicum* R (JCM18229) (17) and recombinant strains were precultured at 33°C overnight in nutrient-rich medium (A medium) containing (per liter) 2 g of urea, 2 g of yeast extract, 7 g of Casamino Acids, 7 g of (NH<sub>4</sub>)<sub>2</sub>SO<sub>4</sub>, 0.5 g of KH<sub>2</sub>PO<sub>4</sub>, 0.5 g of K<sub>2</sub>HPO<sub>4</sub>, 0.5 g of MgSO<sub>4</sub> · 7H<sub>2</sub>O, 6 mg of FeSO<sub>4</sub> · 7H<sub>2</sub>O, 4.2 mg of MnSO<sub>4</sub> · H<sub>2</sub>O, 0.2 mg of biotin, and 0.2 mg of thiamine, supplemented with 4% (wt/vol) glucose (10). Where appropriate, the medium was supplemented with antibiotics. The final antibiotic concentrations were as follows: for *E. coli*, 50 μg ml<sup>-1</sup> of ampicillin and 50 μg ml<sup>-1</sup> of kanamycin, and for *C. glutamicum*, 50 μg ml<sup>-1</sup> of kanamycin.

To investigate the growth performance of *C. glutamicum* under aerobic conditions, recombinant strains were harvested by centrifugation

(5,000 × g at room temperature for 5 min). Cell pellets were subsequently washed twice with mineral medium (BT medium) containing (per liter) 7 g of (NH<sub>4</sub>)<sub>2</sub>SO<sub>4</sub>, 0.5 g of KH<sub>2</sub>PO<sub>4</sub>, 0.5 g of K<sub>2</sub>HPO<sub>4</sub>, 0.5 g of MgSO<sub>4</sub> · 7H<sub>2</sub>O, 6 mg of FeSO<sub>4</sub> · 7H<sub>2</sub>O, 4.2 mg of MnSO<sub>4</sub> · H<sub>2</sub>O, 0.2 mg of biotin, and 0.2 mg of thiamine. After the second wash, cells were resuspended in 10 ml of BT medium containing an appropriate concentration of sugars. The resulting mixture was incubated at 33°C with constant agitation (200 rpm) in a test tube.

**DNA manipulations.** Plasmid DNA was isolated by using a NucleoSpin plasmid kit (TaKaRa) according to the manufacturer's instructions. PCR was performed with KAPA *Taq* Extra polymerase (Nippon Genetics) or PrimeStar GXL DNA polymerase (TaKaRa) using a GeneAmp PCR system (Applied Biosystems, Foster City, CA). Oligonucleotide primers used in this study are listed in Table 2. The resultant PCR fragments were purified with NucleoSpin Gel and PCR Clean-Up kit (TaKaRa) according to the manufacturer's instructions.

*Corynebacteria* were transformed by electroporation as previously described (18). Transformation of *E. coli* was performed by the CaCl<sub>2</sub> procedure (16).

**DNA sequencing.** All sequencing was performed by the dideoxy chain termination method as previously described (19) with an ABI Prism 3100 genetic analyzer (Applied Biosystems) using a BigDye Terminator, version 3.1, cycle sequencing kit (Applied Biosystems). DNA sequence data were analyzed with the Genetyx program (Software Development, Tokyo, Japan). Database searches were performed using the BLAST server of National Center for Biotechnology Information (<http://www.ncbi.nlm.nih.gov>).

TABLE 2 Oligonucleotides used in this study

Primer name	Sequence (5'–3') <sup>a</sup>	Cohesive end
DPXF	CACGAGGA(A/G)TG(C/G)CT(C/G)(A/G)C(C/G)GG	
DPXR	CG(G/C)TG(G/C)GA(G/C)TT(T/C)GTGAAGC(G/A)G	
DPMF	CG(C/G)GACATCGC(A/C)ATGGT(G/T)TTCCAGA	
DPMR	CAGCG(A/G)CCGAAGTAGCCGAG	
APF	TCCGAGCGTTGCATGACCACAGTAAGCTATCACGTAC	
AP-NotIR	GGCCGTACGTGATAGCTTAC	
AP-BamHIR	GATCGTACGTGATAGCTTAC	
AP-MluIR	CGCGGTACGTGATAGCTTAC	
A P1	CCGAGCGTTGCATGACCACAGTAAGCT	
AP2	CGTTGCATGACCACAGTAAGCTATCACGTA	
GWR1-R2	CGCCCATCTCGGCGACGAGGTC	
GWR1-R1	AGCCCCTGGTGGATCCCGAGCTC	
GWF1-F2	CGTCGACGAGTGCATCGCCGAGGA	
GWF1-F1	GCCGCGATCGGCGACACGATGC	
GWR2-R2	CGATTGAAACACGGCCGTGTCGACC	
GWR2-R1	GCGAAGACGAGATGTCATCGCTCAC	
CAmsi-R2	GGCGATCTTGAGCGCAAGCCCATG	
CAmsi-R1	ACCCGAGAGGGCCTTCGGCTTGC	
CAmsi-F2	CGACCGCATCGCGGTCCCTCAAGGA	
CAmsi-F1	CCTCGGCGTACCACGGTCTACG	
Primer 1	GCCGGCAACC <u>CATATG</u> ACCGAACTGCCCCCTCT	NdeI
Primer 2	GGG <u>TACCT</u> CAGCTGACGGGTGCCTCGGCC	KpnI
Primer 3	GGGAATTCCATATGAGAGCACACAGGATCCTGACG	NdeI
Primer 4	GGGGTACCACGGATCGTTCCGGCACGTAC	KpnI
Primer 5	GGGGTACC <u>TTA</u> AGGGAGGCTCTTGCCAG	KpnI
Primer 6	GCGGTACCACTACGGATCGTCCGGCACGTA	KpnI
Primer 7	CCGGTACC <u>TTA</u> CGCCGAGACGATCGCCCTTG	KpnI
Primer 8	GGAATTCCATATGAGGAAAAAGTGTAGCGTATGTTTA	NdeI
Primer 9	GAAGATCTCTATCTTTGCGTAAACTGCCAG	BglII
Primer 10	AGGAAAGATCTCAGCTGACGGGTGCCTCGGCC	BglII
CgR2369_d1F	GCTCTAGAAAGGAACATCGTCATCGACCTTG	XbaI
CgR2369_d1R	GACAAAGCCCGGAAGCCATG	
CgR2369_d2F	CATGGCTTCCGGGCTTTGTCTACCCCGAGGCACGTAATG	
CgR2369_d2R	GCTCTAGAGCGGCAGTAACGACCTTGAC	XbaI

<sup>a</sup> The restriction site overhangs used in the cloning procedure are underlined.

**Degenerate PCR and adaptor ligation PCR.** Chromosomal DNA was isolated from *C. alkanolyticum* by using Wizard SV Mini Preps (Promega) according to the manufacturer's instructions. Degenerate nested PCRs were performed using *C. alkanolyticum* chromosomal DNA as the template with the degenerate primers to generate core DNA fragments which were homologous to known bacterial  $\beta$ -xylosidase genes or *msiK* genes. The degenerate PCR primers for the  $\beta$ -xylosidase gene were DPXF and DPXR, and those for the *msiK* gene were DPMF and DPMR (Table 2). The resultant core fragments were ligated to pGEM-T Easy vector (Promega), and their nucleotide sequences were analyzed. The nucleotide sequences upstream and downstream of the core fragments were obtained by chromosome walking using the adaptor ligation PCR method (20). *C. alkanolyticum* chromosomal DNA was digested with a single restriction enzyme, such as BglII, MluI, or NotI, followed by ligation with the adaptor DNA constituted by oligonucleotides APF and AP-BamHR, AP-MluIR, or AP-NotIR (Table 2), which contained PCR primer sequences. After ligation, nested PCR was performed using the ligation product as the template with the gene-specific primers and the adaptor primers AP1 for the first PCR and AP2 for the nested PCR (Table 2). The gene-specific primers GWF1-F1, GWF1-F2, GWR1-R1, GWR1-R2, GWR2-R1, and GWR2-R2 for cloning of the *xylEFGDHR* gene cluster and the gene-specific primers CAmsi-F1, CAmsi-F2, CAmsi-R1, and CAmsi-R2 for cloning the *msiK* gene are listed in Table 2. Resultant PCR fragments were inserted into pGEM-T Easy vector (Promega), and their nucleotide sequences were analyzed.

**Vectors.** *E. coli*-*C. glutamicum* shuttle vector pCRB52T was constructed as follows. *Ltac5* vector derived from pHSG298 and pCASE1 harboring the *tac* promoter was digested with BamHI, and the 0.7-kb fragment containing the *tac* promoter and terminator was ligated to BamHI- and BglII-digested pCRB52G vector derived from pHSG298 and pBY503. The resultant vector was digested with NdeI and ligated with a linker DNA containing a KpnI site, yielding vector pCRB52T (Table 1).

**Construction of recombinant plasmids.** The 2.4-kb *C. alkanolyticum* *xylD* gene was amplified using *C. alkanolyticum* chromosomal DNA as the template and the oligonucleotides primer 1 and primer 2 (Table 2) to generate a DNA fragment with NdeI and KpnI cohesive ends. The PCR amplicon was subsequently ligated to NdeI- and KpnI-digested pCRB52T, yielding plasmid pCRF100 (Table 1). The 5.6-kb *C. alkanolyticum* *xylEFGD* operon was amplified using the oligonucleotides primer 2 and primer 3 (Table 2) to generate a DNA fragment with NdeI and KpnI cohesive ends. The PCR amplicon was subsequently ligated to NdeI- and KpnI-digested pCRB52T, yielding plasmid pCRF101 (Table 1). The 1.1-kb *C. glutamicum* *cgR\_2369* gene was amplified using the oligonucleotides primer 4 and primer 5 (Table 2) to generate a DNA fragment with KpnI cohesive ends. The PCR amplicon was subsequently ligated to KpnI-digested pCRF101, yielding plasmid pCRF102 (Table 1). The 1.1-kb *C. alkanolyticum* *msiK* gene was amplified using the oligonucleotides primer 6 and primer 7 (Table 2) to generate a DNA fragment with KpnI cohesive ends. The PCR amplicon was subsequently ligated to KpnI-digested pCRF101, yielding plasmid pCRF103 (Table 1). The 1.5-kb arabinoxylan

arabinofuranohydrolase (AXH) gene of *Bacillus subtilis* was amplified using the oligonucleotides primer 8 and primer 9 (Table 2) to generate a DNA fragment with NdeI and BglII cohesive ends. The PCR amplicon was subsequently ligated to NdeI- and BglII-digested pCRB52T, yielding plasmid pCRF105 (Table 1). To express the His<sub>6</sub>-tagged XylD protein, the 2.4-kb *xylD* gene was amplified using *C. alkanolyticum* chromosomal DNA as the template and the oligonucleotides primer 1 and primer 10 (Table 2) to generate a DNA fragment with NdeI and BglII cohesive ends. The PCR amplicon was subsequently ligated to NdeI- and BamHI-digested pColdII vector (TaKaRa), yielding plasmid pCRF106 (Table 1).

**Purification and kinetic analysis of the XylD protein.** To express the His<sub>6</sub>-tagged XylD protein, *E. coli* BL21(DE3) strain was transformed with the plasmid pCRF106. The resultant strain was first grown at 37°C in LB medium containing 50 µg ml<sup>-1</sup> of ampicillin to an optical density at 600 nm (OD<sub>600</sub>) of 0.5 and then grown at 15°C in the presence of 0.5 mM isopropyl-β-D-thiogalactopyranoside (IPTG) for induction for another 24 h. The cells were collected by centrifugation and resuspended with the lysis buffer (100 mM Tris-HCl [pH 8.0], 0.5 M NaCl, 25 mM imidazole, 10 mM 2-mercaptoethanol), followed by sonication. The cell debris was removed by centrifugation, and the cell lysate was applied on a nickel-nitrilotriacetic acid (NTA) column. The column was washed with the wash buffer (100 mM Tris-HCl [pH 8.0], 0.5 M NaCl, 25 mM imidazole), and then protein was eluted with the elution buffer (100 mM Tris-HCl [pH 8.0], 0.5 M NaCl, 250 mM imidazole). The eluent was buffer exchanged to buffer A (20 mM NaP<sub>i</sub> [pH 7.0], 1 mM EDTA, 5 mM MgCl<sub>2</sub>) and subsequently applied to a 1-ml HiTrap Q HP column. The protein was eluted in a linear gradient of sodium chloride to 1.0 M. The purification procedure on the HiTrap Q HP column was performed using an AKTA fast-protein liquid chromatography (FPLC) system (GE Healthcare). The purified XylD protein was subjected to SDS-polyacrylamide gel electrophoresis (PAGE), and its homogeneity was confirmed. The protein concentration was determined using a Bio-Rad protein assay kit.

Kinetic analysis was performed at 33°C in 1 ml of 100 mM HEPES (pH 7.0) solution containing *p*-nitrophenyl-β-D-xylopyranoside (0.04, 0.1, 0.4, 0.8, or 2 mM) or *p*-nitrophenyl-α-L-arabinofuranoside (0.2, 0.4, 1.0, 2.0, or 4.0 mM). Reactions were initiated by the addition of 1 µg of the purified enzyme, and absorbance was measured at 410 nm using a Beckman DU800 spectrophotometer (Beckman Coulter, Inc., Fullerton, CA). To determine the *K<sub>i</sub>* value for xylose, assays were performed at 33°C in 1 ml of 100 mM HEPES (pH 7.0) containing *p*-nitrophenyl-xylopyranoside (0.4, 0.8, 1.2, or 2.0 mM) solution in the presence of xylose (40, 60, 80, or 100 mM). Reactions were initiated by the addition of 1 µg of the purified enzyme, and absorbance was measured at 410 nm. To examine the inhibitory effects of glucose, xylose, and arabinose on XylD activity, assays were performed at room temperature in 0.1 ml of 100 mM HEPES (pH 7.0) containing 1 mM *p*-nitrophenyl-xylopyranoside solution in the presence of each sugar (0, 50, 100, 150, or 200 mM) on a 96-well microtiter plate. Reactions were initiated by the addition of 0.1 µg of the purified enzyme, and absorbance was measured at 410 nm using SpectraMax M2<sup>e</sup> (Molecular Devices).

**Enzyme assays.** For enzyme assay of recombinant strains, cultures were harvested by centrifugation, and cell pellets were washed twice with extraction buffer (100 mM HEPES, pH 7.0). The resulting cell suspensions were homogenized with glass beads for 20 30-s periods, interrupted by 30-s cooling intervals. Cell debris was removed by centrifugation, and the cell lysates were subsequently used as crude extracts for enzyme assays. Enzyme assays were performed in 0.5 ml of reaction mixture (50 mM HEPES [pH 7.0], 1 mM *p*-nitrophenyl-xylopyranoside) at 33°C for 10 min. Reactions were stopped by the addition of 0.5 ml of 50 mM NaOH, and enzyme activities were measured at 410 nm. One unit of enzyme activity was defined as the amount of activity necessary to release 1 µmol of *p*-nitrophenol per min.

**Construction of the *cgR\_2369* deletion mutant.** Deletion of the *cgR\_2369* gene was achieved via a markerless system using suicide vector pCRA725 carrying the *sacB* gene (11). A 1.5-kb DNA fragment just up-

stream of the start codon of the *cgR\_2369* gene and a 1.5-kb DNA fragment just downstream of the stop codon were amplified by PCR using the primer pair CgR2369\_d1F/CgR2369\_d1R and the pair CgR2369\_d2F/CgR2369\_d2R, respectively. Both fragments were combined by overlap extension PCR. The resultant fragment was digested with XbaI and cloned into pCRA725, yielding pCRF1104. *C. glutamicum* X1 was transformed by electroporation with pCRF104, and screening for the deletion mutants was performed as described previously (21). Deletion of the *cgR\_2369* gene was checked by PCR. The mutant strain obtained, X1 Δ*cgR\_2369*, was designated X1(Δ2369).

**Analytical procedure.** Samples were centrifuged (10,000 × *g* at 4°C for 10 min), and the resulting supernatants were analyzed for the presence of sugars. Sugar concentrations were determined by high-performance liquid chromatography (HPLC) using an apparatus (8020; Tosoh Corporation) equipped with a refractive index detector and an HPX-87P column (Bio-Rad) operating at 85°C with a water mobile phase at a flow rate of 0.6 ml min<sup>-1</sup>. Cell mass was determined by measuring the optical density at 610 nm (OD<sub>610</sub>) using a spectrophotometer (DU800; Beckman Coulter, Inc.).

Oligosaccharide profiles in culture medium and cell extract were determined by liquid chromatography-electrospray ionization-mass spectrometry (LC-ESI-MS). For analysis of culture medium, samples were centrifuged (10,000 × *g* at 4°C for 10 min), and the supernatants were diluted 10-fold, followed by mixing with four volumes of acetonitrile. After centrifugation again, the resultant supernatants were analyzed. For analysis of cell extract, 300-samples were centrifuged (10,000 × *g* at 4°C for 10 min), and the cell pellets were washed with 1 ml of water twice and then resuspended with 50 µl of water and extracted by the addition of 200 µl of acetonitrile. After a 30-min incubation on ice, samples were centrifuged (10,000 × *g* at 4°C for 10 min), and the resultant supernatants were analyzed. The chromatographic separations were performed using an apparatus (Shimadzu Corporation) and a TSKgel Amide-80 column (4.5 cm by 0.2 mm; Tosoh Corporation) operating at 60°C with a linear gradient of 75 to 35% buffer B (buffer A, 10 mM ammonium acetate, aqueous; buffer B, acetonitrile) at a flow rate of 0.2 ml min<sup>-1</sup>. LC and MS analyses were controlled using an AB SCIEX QTRAP 5500 LC-tandem MS (LC-MS/MS) system (Applied Biosystems/MDS Analytical Technologies). Negative ions were detected. Authentic xylooligosaccharides were purchased from Megazyme.

**Nucleotide sequence accession numbers.** The nucleotide sequences of the *C. alkanolyticum* *msiK* gene, the gene cluster containing the *xylH* and *xylEFGD* genes, and the *xylR* gene have been deposited in the GenBank database under the accession numbers KM066602, KM066603, and KM066604, respectively.

## RESULTS

**The *C. alkanolyticum* *xylEFGD* gene cluster for xylooligosaccharide metabolism is widely conserved.** Bacterial xylooligosaccharide metabolism involves sugar uptake by xylooligosaccharide transporters prior to hydrolysis by intracellular β-xylosidases, but functional characterization of the genes involved in xylooligosaccharide metabolism in corynebacteria is not known. Nevertheless, knowing that *Corynebacterium alkanolyticum* ATCC 21511 (7, 8) is able to grow in the presence of xylooligosaccharide as the sole carbon source facilitated the cloning of β-xylosidase and xylooligosaccharide transporter genes using degenerate primers, DPXF and DPXR (Table 2), designed from highly conserved regions of β-xylosidases of actinobacteria. Subsequent degenerate PCR using *C. alkanolyticum* chromosomal DNA as the template revealed a 360-bp core DNA fragment encoding a polypeptide homologous to bacterial β-glycosidase. DNA fragments upstream (GWR1 and GWR2) and downstream (GWF1) of this core fragment (Fig. 1A) were obtained by chromosome walking based on the adaptor ligation PCR method (20). An approximately 9-kb region of the *C.*



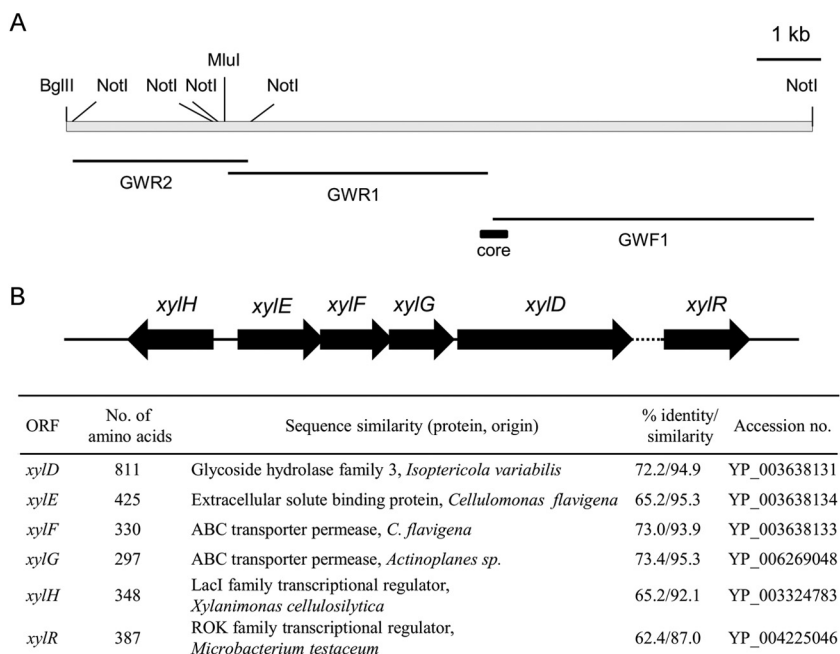


**FIG 1** The *C. alkanolyticum* gene cluster for xylooligosaccharide utilization. (A) Physical map of the cluster indicating restriction sites for MluI, NotI, and BglII used in construction of a genomic DNA library for chromosome walking. The three fragments determined by the chromosome walking (thin solid bars) are depicted relative to the core fragment (thick solid bar). (B) Organization of genes on the cluster. The region whose nucleotide sequence could not be determined (dotted line) is located between *xylD* and *xylR*. Accession numbers are given at right.

*alkanoliticum* chromosome containing the gene fragment homologous to  $\beta$ -glycosidase was thus sequenced to reveal a G+C content of 71.4%, which is well above the genomic G+C content of corynebacteria of 51 to 65%. The region encompasses six predicted complete open reading frames (ORFs), *xylH*, *xylR*, *xylE*, *xylF*, *xylG*, and *xylD*, with each of *xylE*, *xylF*, and *xylG* overlapping its neighbor (Fig. 1B). A segment not exceeding 100 bp between *xylD* and *xylR* could not be sequenced, suggesting the possibility of a long palindromic sequence. A BLAST search (Fig. 1B) strongly suggested that *xylE* encodes a putative sugar ABC transporter solute-binding protein, whereas *xylF* and *xylG* encoded putative sugar ABC transporter permeases, with the trio collectively comprising a sugar ABC transporter. The putative solute-binding protein encoded by *xylE* showed highest homology to the extracellular solute-binding protein of *Cellulomonas flavigena* but weak homology (27.9% identity at the amino acid level) to *Streptomyces thermoviolaceus* BxlE (5), a confirmed solute-binding protein of a xylooligosaccharide ABC transporter. *xylD* encoded a putative glycoside hydrolase family 3 protein, with highest homology to that of *Isoptericola variabilis* but lower homology (26.5% identity at the amino acid level) to *S. thermoviolaceus*  $\beta$ -xylosidase BxlA (22). As no signal sequence associated with the putative *xylD*-encoded protein was detected, the gene was predicted to encode an intracellular enzyme. *xylH* and *xylR* encoded putative proteins bearing high homology to the Lacl type transcription factor and ROK (repressor or kinase) family transcription factor, respectively.

To determine the enzymatic properties of the *xylD*-encoded protein, the protein was fused with a His<sub>6</sub> tag at its N terminus, expressed in *E. coli*, purified by a Ni-NTA-Sepharose column and anion exchange chromatography, and confirmed to be homogeneous by SDS-PAGE. XylD's optimal pH for activity at 33°C was

7.0. Its Michaelis constant ( $K_m$ ) was  $2.4 \pm 0.1$  mM toward *p*-nitrophenyl- $\beta$ -D-xylopyranoside (*p*NPX) and  $44.0 \pm 9.0$  mM toward *p*-nitrophenyl- $\alpha$ -D-arabinofuranoside (*p*NPA). Its maximum velocity ( $V_{max}$ ) was  $0.06 \pm 0.01$   $\mu\text{mol s}^{-1} \mu\text{g}^{-1}$  toward *p*NPX and  $1.3 \pm 0.1$   $\mu\text{mol s}^{-1} \mu\text{g}^{-1}$  toward *p*NPA. Its turnover number was  $111 \pm 4$   $\text{s}^{-1}$  toward *p*NPX and  $5 \pm 1$   $\text{s}^{-1}$  toward *p*NPA. The XylD activity toward *p*NPX was inhibited by xylose and arabinose but not glucose (Fig. 2). Xylose was a more potent inhibitor of XylD than arabinose. Arabinose at 200 mM reduced XylD activity by approximately 40%, while 200 mM xylose reduced XylD activity by approximately 70%. End-product inhibi-

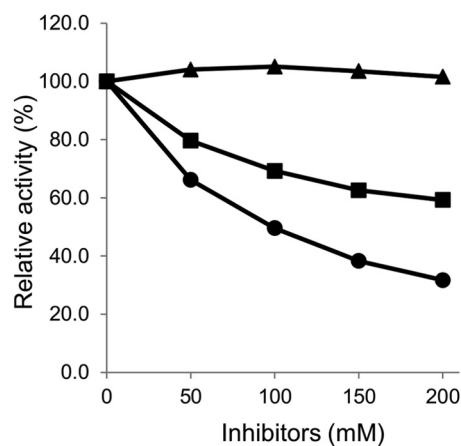


**FIG 2** Inhibitory effects of various sugars on XylD activity. XylD was incubated with *p*NPX in the presence of each sugar (0, 50, 100, 150, and 200 mM), and  $\beta$ -xylosidase activities were compared by initial velocity. The data represent the averages of triplicate experiments. ▲, glucose; ●, xylose; ■, arabinose.

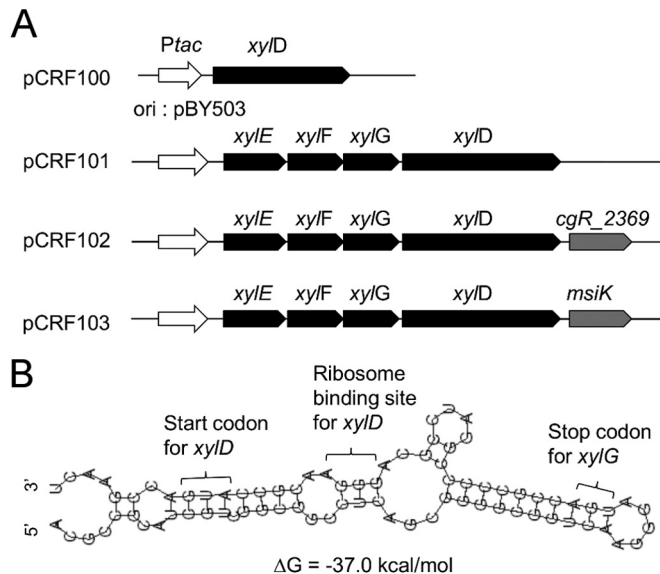


**FIG 3** Plasmids for heterologous expression of *xylEFGD* genes in *C. glutamicum*. (A) Architecture of expression cassettes on *xylD*-harboring plasmid pCRF100, *xylEFGD*-harboring plasmid pCRF101, *xylEFGD*- and *cgR\_2369*-harboring plasmid pCRF102, and *xylEFGD*- and *msiK*-harboring plasmid pCRF103. All plasmid genes are under the control of the strong constitutive *tac* promoter. Each expression cassette is on the *C. glutamicum*-*E. coli* shuttle vector where the corynebacterial replication of origin is from plasmid pBY503. (B) Secondary structure of the translation initiation region of the *xylD* gene as predicted by the RNAfold WebServer (<http://rna.tbi.univie.ac.at/cgi-bin/RNAfold.cgi>).

tion of activity in the presence of pNPX as the substrate was competitive, with an inhibition constant ( $K_i$ ) for xylose of  $67.6 \pm 2.6$  mM.

***C. glutamicum* X1EFGD xylosidase activity and xylooligosaccharide transport are independent.** *C. glutamicum* X1 is a xylose-utilizing strain by virtue of harboring *E. coli* *xylA* encoding xylose isomerase and *xylB* encoding xylulokinase (9). The well-acknowledged merits that *C. glutamicum* possesses as a mixed-sugar-utilizing bacterium provided motivation for heterologous expression of the *xylEFGD* gene cluster in strain X1 in order to determine the functional characteristics of the cluster. Strain X1 transformed with plasmid pCRF100 harboring the *xylD* gene was designated X1D, whereas strain X1 transformed with plasmid pCRF101 harboring the *xylEFGD* gene cluster was designated X1EFGD. A *cgR\_2369* disruption strain of X1 similarly transformed with pCRF100 yielded X1( $\Delta$ 2369)D, whereas X1 transformed with pCRF101 yielded X1( $\Delta$ 2369)EFGD. *C. glutamicum* *cgR\_2369* exhibits high homology to the *Streptomyces* *msiK* gene encoding a multitask ATP-binding protein that assists different oligosaccharide ABC transporters (23). The genes carried by each plasmid used in the transformation were expressed under the control of the strong constitutive *tac* promoter (Fig. 3A). As per expectations, no xylosidase activity was detected with strain X1 due to its lack of an *xylD* gene. Less obvious was the observation that the  $\beta$ -xylosidase activities of strains transformed with pCRF101 were consistently 10-fold weaker than those of corresponding strains transformed with pCRF100, irrespective of the presence of the *cgR\_2369* gene (Table 3). It follows that in strains transformed with pCRF101, XylD translation from *xylEFGD* mRNA exhibiting

a stable secondary structure predicted around the translation initiation site of the *xylD* gene (Fig. 3B) was not efficient.

The relative abilities of strains X1, X1D, and X1EFGD to utilize xylooligosaccharides was assayed by monitoring growth and sugar consumption in rich medium supplemented with a 0.25% (wt/vol) commercial xylooligosaccharide mixture. The HPX-87P HPLC column employed permitted resolution of xylose and xylobiose but not higher xylooligosaccharides. The maximum cell density ( $OD_{610}$ ) was 2.4 with strain X1, 3.9 with strain X1D, and 4.3 with strain X1EFGD (Fig. 4A). Given the earlier mentioned inability of any of the strains to grow in minimal medium, the growth of strain X1 in rich medium observed here must be attributed to carbon sources other than the xylooligosaccharide mixture. HPLC analysis confirmed that strain X1 did not utilize xylobiose, and no xylose was detected in its culture medium (Fig. 4B). In contrast, rapid consumption of 30% of the initial xylobiose by strain X1D and of 95% by strain X1EFGD in 12 h was mirrored by comparative differences in xylose accumulation in both strains. Thereafter, xylobiose consumption by strain X1D decreased to such an extent that after 24 h about 55% of the xylobiose remained. Xylose, too, was gradually utilized by both strains during the latter phase. The higher proficiency of strain X1EFGD with respect to xylobiose utilization must reside in the role played by an *xylEFG* gene product.

***C. glutamicum* *cgR\_2369* gene product facilitates xylooligosaccharide transport.** The expression of the *xylEFGD* operon alone was enough to affect efficient uptake of xylooligosaccharides in *C. glutamicum*. This suggested that an ATP binding protein known to assist the XylEFG activity is expressed independently in *C. glutamicum*. The gene organization of the *xylEFG* cluster is conserved in many species (5, 6, 24). In *Streptomyces* species, *msiK* encodes a multitask ATP-binding protein that assists different oligosaccharide ABC transporters (23). The *C. glutamicum* R *cgR\_2369* putative gene product highly homologous to the *msiK* product (58.9% amino acid identity to *Streptomyces reticuli* MsiK) is located apart from any ABC transporter-encoding gene cluster on the chromosome, as is characteristic of *msiK* genes. The effect, if any, of the *cgR\_2369* gene product on XylEFG was assayed using a *cgR\_2369* deletion mutant. The *cgR\_2369* gene was deleted from strain X1 using a markerless system to yield strain X1( $\Delta$ 2369). Strain X1( $\Delta$ 2369) transformed with pCRF100 was designated X1( $\Delta$ 2369)D, whereas X1( $\Delta$ 2369) transformed with pCRF101 was designated X1( $\Delta$ 2369)EFGD (Table 1). The  $\beta$ -xylosidase activities of strain X1( $\Delta$ 2369)D and X1( $\Delta$ 2369)EFGD were unchanged from those of strain X1D and X1EFGD, respectively (Ta-

**TABLE 3**  $\beta$ -Xylosidase activities in *C. glutamicum* recombinant strains

Strain	Specific activity (U/mg of protein) <sup>a</sup>
X1	ND
X1D	0.2561 $\pm$ 0.0026
X1EFGD	0.0282 $\pm$ 0.0003
X1( $\Delta$ 2369)D	0.2565 $\pm$ 0.0015
X1( $\Delta$ 2369)EFGD	0.0274 $\pm$ 0.0002
X1( $\Delta$ 2369)EFGDK	0.0292 $\pm$ 0.0001
X1( $\Delta$ 2369)EFGDM	0.0284 $\pm$ 0.0002

<sup>a</sup> Cells were grown aerobically to late log phase in A medium containing 40 g liter<sup>-1</sup> glucose with 50 mg ml<sup>-1</sup> kanamycin. The reported data represent the averages calculated from triplicate measurements. ND, no activity detected.

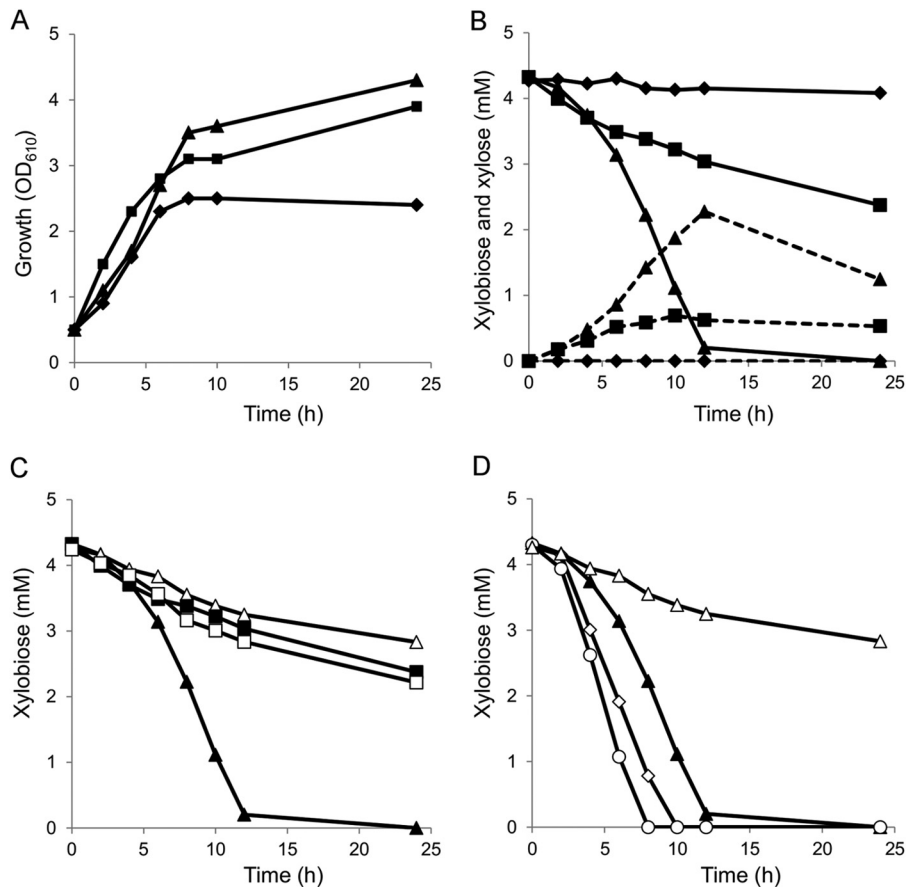


**FIG 4** Growth and pentose sugar consumption of *C. glutamicum* recombinant strains precultured in nutrient-rich A medium containing 40 g liter<sup>-1</sup> glucose, inoculated to an initial OD<sub>610</sub> of 0.5 in A medium containing 2.5 g liter<sup>-1</sup> xylooligosaccharide mixture. Xylobiose consumption levels in the recombinant strains were analyzed by HPLC. (A) Aerobic growth of strain X1 (◆), strain X1D (■), and strain X1EFGD (▲). (B) Sugar consumption of strain X1 (◆), strain X1D (■), and strain X1EFGD (▲). Solid and dashed lines indicate the concentrations of xylobiose and xylose, respectively. (C) Comparison of xylobiose consumption levels of strain X1(Δ2369)D (□) and X1(Δ2369)EFGD (△) with those of strains X1D (■) and X1EFGD (▲). (D) Comparison of xylobiose consumption levels of strains X1(Δ2369)EFGDK (○) and X1(Δ2369)EFGDM (◇) with those of strains X1EFGD (▲) and X1(Δ2369)EFGD (△). Xylobiose concentration was represented as the concentration of xylose per unit. The data represent the averages of triplicate experiments.

ble 4). However, whereas strain X1(Δ2369)D consumed xylobiose at the same rate as strain X1D, strain X1(Δ2369)EFGD's initial rate of xylobiose consumption was only 17% of the 0.344 mM/h rate observed with strain X1EFGD (Fig. 4C).

To confirm the role of *cgR\_2369*, the *cgR\_2369* gene with the 5' untranslated region was inserted just downstream of *xylD* on plasmid pCRF101 so as to express the *xylEFGD* and *cgR\_2369* genes polycistronically under the control of the *tac* promoter, and strain X1(Δ2369)EFGD was complemented with the *cgR\_2369* gene of *C. glutamicum*. The resultant plasmid pCRF102 (Fig. 2) was used to transform strain X1(Δ2369) to strain X1(Δ2369)EFGDK (Table 1). The β-xylosidase activity of strain X1(Δ2369)EFGDK was comparable to the activities of strains X1EFGD and X1(Δ2369)EFGD (Table 4), but its xylooligosaccharide consumption was restored to the levels observed with strain X1EFGD (Fig. 4D).

To obtain a native *msiK* gene of *C. alkanolyticum*, degenerate primers DPMF and DPMR (Table 2) were designed from the highly conserved region of actinobacterial *msiK* genes. Degenerate PCR using *C. alkanolyticum* chromosomal DNA as the template gave a 480-bp core DNA fragment encoding a polypeptide highly homologous to actinobacteria *msiK*. Subsequent DNA fragments

upstream and downstream of the core fragment were obtained by chromosome walking, and the complete ORF of *msiK* was determined. The protein deduced thereof shared 83% amino acid identity in the N-terminal 240-amino-acid portion and 67% amino acid identity overall with *S. reticuli* MsiK. To coexpress *msiK* with the *xylEFGD* cluster, the *msiK* gene with the ribosome binding site was inserted just downstream of *xylD* on plasmid pCRF101 so as to express the *xylEFGD* and the *msiK* genes polycistronically under the control of the *tac* promoter. The resultant plasmid pCRF103 (Fig. 2) was used to transform strain X1(Δ2369) to strain X1(Δ2369)EFGDM (Table 1). The β-xylosidase activity of strain X1(Δ2369)EFGDM was comparable to the activities strains X1EFGD and X1(Δ2369)EFGD (Table 4), but its xylooligosaccharide consumption was restored to the levels observed with strain X1EFGD (Fig. 4D).

**The *xylEFG* product transports arabino-xylooligosaccharides as well as xylooligosaccharides.** LC-ESI-MS analysis with a TSKgel Amide-80 column showed that the commercial xylooligosaccharide mixture used in this study contained xylobiose (X2), xylotriose (X3), xylotetraose (X4), and unknown pentose oligosaccharides with degrees of polymerization of 4, 5, and 6 (P4, P5,

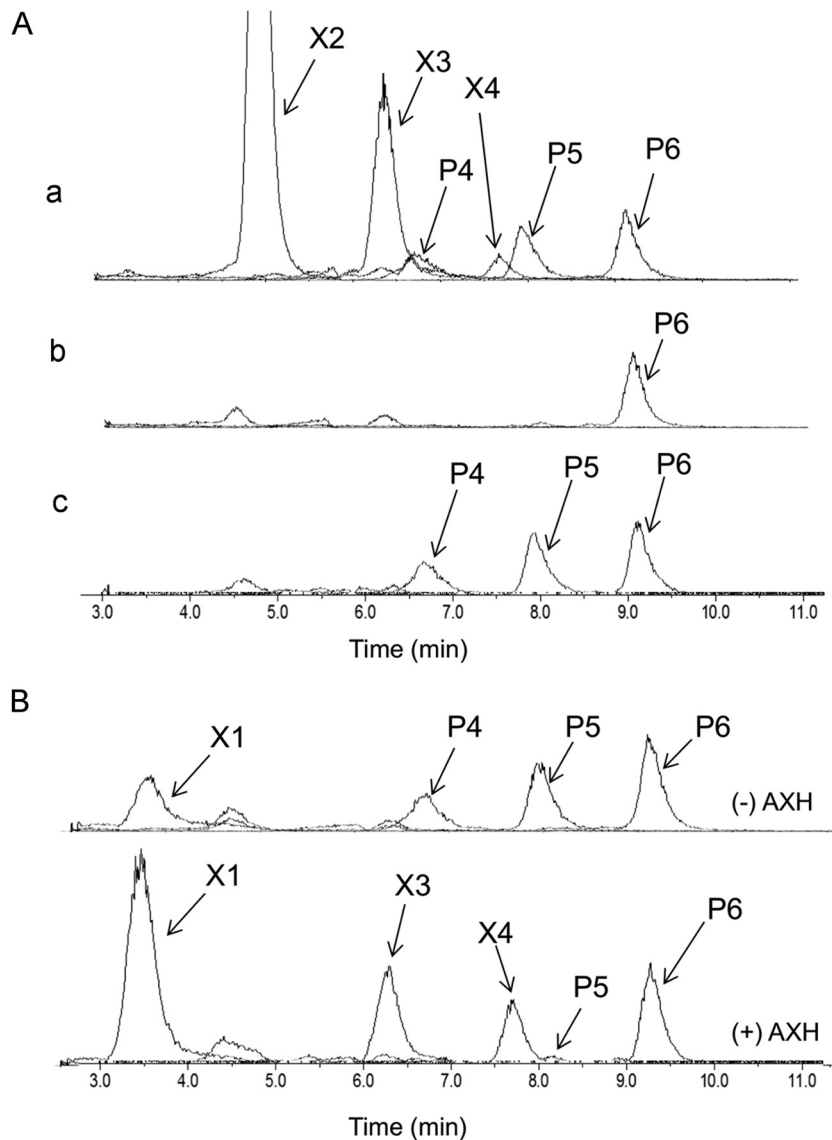


**FIG 5** Comparison of substrate utilization range of *C. glutamicum* recombinant strains. Strain X1EFGD and strain X1D were first grown aerobically to late log phase in A medium containing  $40 \text{ g liter}^{-1}$  of glucose and then inoculated to an initial  $\text{OD}_{610}$  of 0.5 into A medium containing  $2.5 \text{ g liter}^{-1}$  of xylooligosaccharide mixture. (A) Culture medium of the recombinant strains was analyzed by LC-ESI-MS at 0 h (a), at 30 h for strain X1EFGD (b), and at 120 h for strain X1D (c) after the start of cultivation. (B) Characterization of oligosaccharides P4 and P5. The culture medium of strain X1D from the experiment represented in panel A, row c, was incubated with or without the cells of strain BsrAXH expressing the extracellular arabinoxylan arabinofuranohydrolase (AXH). After incubation, the samples were centrifuged, and the supernatants were analyzed by LC-ESI-MS. The lower spectrum was from the sample treated with (+) AXH, and the upper one was from the sample without (-) AXH. Compounds P4, P5, and P6 were oligosaccharides whose molecular weights corresponded to pentose-oligosaccharides composed of 4 to 6 pentose units. X2, xylobiose; X3, xylotriose; X4, xylotetraose.

and P6, respectively) (Fig. 5A, row a). The culture medium of each of strain X1D and X1EFGD grown in A medium supplemented with 0.25% (wt/vol) xylooligosaccharide mixture and analyzed by LC-ESI-MS at 24 h or 120 h revealed that, whereas strain X1EFGD was able to completely consume all but P6 (Fig. 5A, row b), strain X1D completely consumed only xylobiose, xylotriose, and xylotetraose (Fig. 5A, row c). This ability of strain X1EFGD to utilize P4 and P5 must therefore be attributed to the *xylEFG* product.

The commercial xylooligosaccharide mixture used in this study is a product of enzymatic hydrolysis of arabinoxylan, implying that the three unknown fractions could be arabino-xylotriose (P4), arabino-xylotetraose (P5), and arabino-xylopentaose (P6).

Confirming the identity of the fractions may indicate why P6 was not consumed, thus revealing the substrate range that the product of *xylEFG* binds. To this end, a strain X1D digest of the xylooligosaccharide mixture (used for the experiment shown in Fig. 5A) was incubated with cells of the *C. glutamicum* recombinant strain BsrAXH (Table 1), a recombinant R strain harboring the gene encoding the extracellular arabinoxylan arabinofuranohydrolase (AXH) from *B. subtilis* (25). A supernatant of the digest thereof analyzed by LC-ESI-MS revealed that P4 and P5 were decomposed to xylotriose and xylotetraose with the release of a pentose monomer (Fig. 5B). Arabinose, being indistinguishable from xylose by TSKgel Amide-80 chromatography, was confirmed by HPLC on



an HPX-87P column (data not shown). These results suggested that P4 and P5 were arabino-xylotri-ose and arabino-xylo-tetraose, respectively. P6 was not decomposed by the treatment with strain BsrAXH, and its chemical structure is still unknown.

**Arabino-xylooligosaccharides were accumulated in the cell in strain X1EFGD.** In strain X1EFGD, uptake of arabino-xylooligosaccharides was not followed by release and accumulation of arabinose although strain X1EFGD had none of the arabinose metabolism genes, such as *araBAD* (arabinose isomerase, ribulokinase, and ribulose-5-phosphate 4-epimerase). When the xylooligosaccharide mixture used in this study was incubated with the purified XylD under the same conditions as used in the enzyme assays, oligosaccharides P4, P5, and P6 were hardly decomposed while xylooligosaccharides were completely decomposed to xylose (data not shown). These results suggested that most of arabino-xylooligosaccharides taken up were accumulated in the cell without any decomposition. To examine the hypothesis, the cell pellets of strain X1EFGD grown in A medium supplemented with 0.25% (wt/vol) xylooligosaccharide mixture were extracted with an acetonitrile-water solution after extensive washing at 24 h. The culture medium and cell extract at 24 h analyzed by LC-ESI-MS revealed that in strain X1EFGD, oligosaccharides P4 and P5 (arabino-xylotri-ose and arabino-xylo-tetraose) absent in culture medium were detected in cell extract, while xylooligosaccharides were fully metabolized, and oligosaccharide P6 present in culture medium was absent from the cell extract (Fig. 6B and C), which indicated that arabino-xylotri-ose and arabino-xylo-tetraose were taken up but not metabolized efficiently. The arabino-xylooligosaccharide composition in the experiment shown in Fig. 6A was different from that in the experiment shown in Fig. 5 as the production lot of the xylooligosaccharide mixture used in this experiment was different from that used in Fig. 5.

## DISCUSSION

Xylooligosaccharides are  $\beta$ -1,4-linked xylose oligomers derived from the hydrolysis of xylan, an important component of cellulosic biomass. Xylanolytic microorganisms secrete enzymes that hydrolyze xylan to its constituent xylooligosaccharides that can then be taken up by cells. In bacteria the xylooligosaccharides are transported into cells by the action of xyloside transporters before subsequent hydrolysis to xylose by the intracellular 1,4- $\beta$ -xylosidases. Most bacterial  $\beta$ -xylosidases and xyloside transporters characterized to date are from *Firmicutes* and *Proteobacteria* (3, 20, 26, 27). Homologues of  $\beta$ -xylosidase and xyloside transporter genes are extensively evident among completely sequenced actinobacterial genomes, but functional characterization of the encoded enzymes is not known except in *Streptomycineae* (5, 22, 28). In this study, the  $\beta$ -xylosidase and xyloside transporter genes of the glutamate- and biosurfactant-producing corynebacterium *C. alkanolyticum* (7, 8) were shown to form a functional cluster exhibiting a 71.4% G+C content that is markedly higher than the typical 51 to 65% of genomes of corynebacteria. The proteins encoded by *xylD* and *xylE* showed high homology to *Cellulomonas flavigena* glycoside hydrolase family 3 proteins and the extracellular solute-binding protein, respectively. Moreover, a partial sequence of 16S rRNA of *C. alkanolyticum* showed the highest homology to that of *Microbacterium testaceum*. Given that both *C. flavigena* and *M. testaceum* are *Micrococcineae*, these similarities betray a closer relationship of *C. alkanolyticum* to *Micrococcineae* than to *Corynebacterineae*.

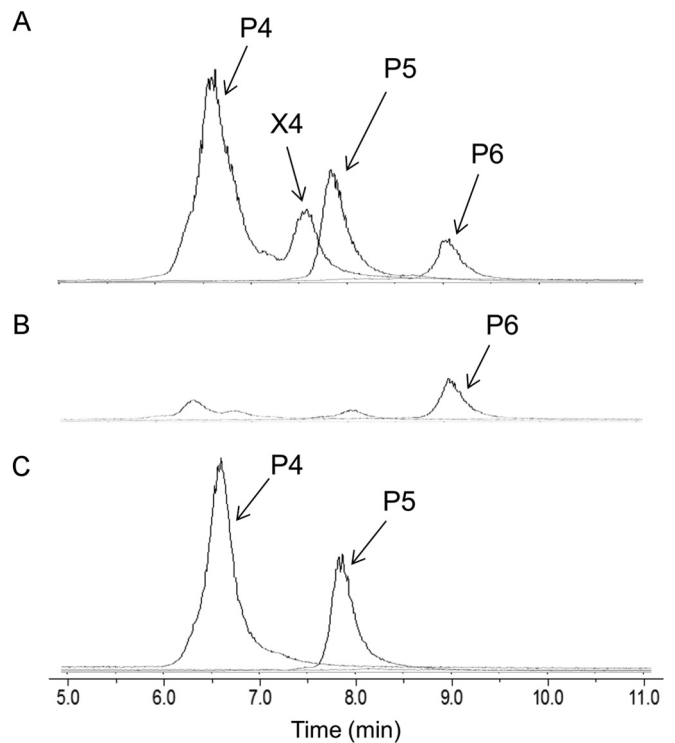


**FIG 6** Detection of intracellular arabino-xylooligosaccharides. Strain X1EFGD was first grown aerobically to late log phase in A medium containing 40 g liter<sup>-1</sup> glucose and then inoculated to an initial OD<sub>610</sub> of 0.5 into A medium containing 2.5 g liter<sup>-1</sup> xylooligosaccharide mixture. (A) Culture medium analyzed by LC-ESI-MS at 0 h. (B) Culture medium analyzed by LC-ESI-MS at 24 h. (C) Cell extract analyzed by LC-ESI-MS at 24 h. For each analysis, negative ions corresponding to pentose oligosaccharides composed of 4 to 6 pentose units were detected. Compounds P4, P5, and P6 were oligosaccharides whose molecular weights corresponded to pentose oligosaccharides composed of 4 to 6 pentose units. X4, xylo-tetraose.

The *xylD*-encoded protein was a typical bacterial  $\beta$ -xylosidase with a moderately high turnover number and high  $K_i$  value for xylose, suggesting an inherent potential for industrial application in a suitable industrial strain. In *C. glutamicum*  $\beta$ -xylosidase activity derived from the unmodified *xylEFGD* cluster was suppressed owing to reduced translation efficiency from a stable secondary structure within the translation initiation region. A similar stable stem-loop structure within the translation initiation region in the  $\beta$ -xylosidase-encoding *xylC* of *Thermoanaerobacterium saccharolyticum* resulting in comparable suppression of activity has been removed by site-directed mutagenesis (29). A similar approach to enhance the *xylEFGD* cluster-derived xylosidase activity may lead to more productive industrial strains. The significance of the translational modification of the *xylD* gene in xylooligosaccharide utilization by *C. alkanolyticum* ought to be explored.

The similar capacity of strain X1D not expressing *xylEFG* to utilize xylobiose suggests the presence of an inherent xylobiose uptake mechanism independent of the *xylEFG*-encoded transporter in *C. glutamicum*. It is clear that a doubling of this capacity occurs only in strains expressing the transporter in the presence of a functional multitask ATP-binding protein. Strains not expressing the transporter were able to utilize xylobiose, xylotri-ose, and xylo-tetraose, but utilization of the more complex arabino-xylotri-ose and arabino-xylo-tetraose required the *xylEFG*-encoded trans-

porter. In strain X1EFGD, arabino-xylotriase and arabino-xylo-tetraose taken up by the *xylEFG*-encoded transporter were hardly metabolized in the cell because of low activity of the *xylD*-encoded  $\beta$ -xylosidase toward them. For efficient utilization of arabino-xylooligosaccharides, coexpression of arabinofuranosidase must be required.

The two other xylooligosaccharide ABC transport systems reported to date have not been functionally characterized beyond demonstration of their substrate binding proteins to exhibit high affinity toward xylooligosaccharides (5, 6). Nevertheless, similarly organized ABC transport-encoding gene clusters, including *S. reticuli cebEFG* for cellobiose (24) and *B. subtilis araNPQ* for arabino-oligosaccharides (30), do require multitask ATP-binding proteins to function. These ATP-binding proteins are invariably encoded by genes distant from the clusters: *msiK* in *S. reticuli* and *msmX* in *B. subtilis*. The successful expression of the xylooligosaccharide ABC transporter gene cluster in a heterologous host in this study demonstrates the central role of the cluster in uptake of arabino-xylooligosaccharides. *C. glutamicum* has been engineered and improved to be an effective platform for pentose fermentation (31–33), producing ethanol (34), succinic acid (35), 1,5-diaminopentane (36), and amino acids (37, 38) from pentose sugars. The findings described here could offer faster, broader, and more efficient pentose sugar utilization to such potential industrial strains, and could contribute significantly to advancement of microbial lignocellulosic biomass exploitation.

## ACKNOWLEDGMENT

We thank Crispinus A. Omumasaba (Research Institute of Innovative Technology for the Earth) for helpful comments on the manuscript.

## REFERENCES

- Aristidou A, Penttilä M. 2000. Metabolic engineering applications to renewable resource utilization. *Curr Opin Biotechnol* 11:187–198. [http://dx.doi.org/10.1016/S0958-1669\(00\)00085-9](http://dx.doi.org/10.1016/S0958-1669(00)00085-9).
- Dodd D, Cann I. 2009. Enzymatic deconstruction of xylan for biofuel production. *Glob Change Biol Bioenergy* 1:2–17. <http://dx.doi.org/10.1111/j.1757-1707.2009.01004.x>.
- Qian Y, Yomano L, Preston J, Aldrich H, Ingram L. 2003. Cloning, characterization, and functional expression of the *Klebsiella oxytoca* xylo-dextrin utilization operon (*xynTB*) in *Escherichia coli*. *Appl Environ Microbiol* 69:5957–5967. <http://dx.doi.org/10.1128/AEM.69.10.5957-5967.2003>.
- Shin H, McClendon S, Vo T, Chen R. 2010. *Escherichia coli* binary culture engineered for direct fermentation of hemicellulose to a biofuel. *Appl Environ Microbiol* 76:8150–8159. <http://dx.doi.org/10.1128/AEM.00908-10>.
- Tsujibo H, Kosaka M, Ikenishi S, Sato T, Miyamoto K, Inamori Y. 2004. Molecular characterization of a high-affinity xylobiose transporter of *Streptomyces thermoviolaceus* OPC-520 and its transcriptional regulation. *J Bacteriol* 186:1029–1037. <http://dx.doi.org/10.1128/JB.186.4.1029-1037.2004>.
- Shulami S, Zaide G, Zolotnitsky G, Langut Y, Feld G, Sonenshein A, Shoham G. 2007. A two-component system regulates the expression of an ABC transporter for xylo-oligosaccharides in *Geobacillus stearothermophilus*. *Appl Environ Microbiol* 73:874–884. <http://dx.doi.org/10.1128/AEM.02367-06>.
- Crosman J, Pinchuk R, Cooper D. 2002. Enhanced biosurfactant production by *Corynebacterium alkanolyticum* ATCC 21511 using self-cycling fermentation. *J Am Oil Chem Soc* 79:467–472. <http://dx.doi.org/10.1007/s11746-002-0507-5>.
- Nakao Y, Kanamaru T, Kikuchi M, Yamatoda S. 1973. Action of penicillin on membrane-permeability barrier to L-glutamic acid. I. Extracellular accumulation of phospholipids, UDP-N-acetylhexosamine derivatives and L-glutamic acid by penicillin-treated *Corynebacterium alkanolyticum*. *Agric Biol Chem* 37:2399–2404.
- Sasaki M, Jojima T, Inui M, Yukawa H. 2008. Simultaneous utilization of D-cellobiose, D-glucose, and D-xylose by recombinant *Corynebacterium glutamicum* under oxygen-deprived conditions. *Appl Microbiol Biotechnol* 81:691–699. <http://dx.doi.org/10.1007/s00253-008-1703-z>.
- Inui M, Murakami S, Okino S, Kawaguchi H, Vertès A, Yukawa H. 2004. Metabolic analysis of *Corynebacterium glutamicum* during lactate and succinate productions under oxygen deprivation conditions. *J Mol Microbiol Biotechnol* 7:182–196. <http://dx.doi.org/10.1159/000079827>.
- Inui M, Kawaguchi H, Murakami S, Vertès A, Yukawa H. 2004. Metabolic engineering of *Corynebacterium glutamicum* for fuel ethanol production under oxygen-deprivation conditions. *J Mol Microbiol Biotechnol* 8:243–254. <http://dx.doi.org/10.1159/000086705>.
- Yamamoto S, Suda M, Niimi S, Inui M, Yukawa H. 2013. Strain optimization for efficient isobutanol production using *Corynebacterium glutamicum* under oxygen deprivation. *Biotechnol Bioeng* 110:2938–2948. <http://dx.doi.org/10.1002/bit.24961>.
- Jojima T, Fujii M, Mori E, Inui M, Yukawa H. 2010. Engineering of sugar metabolism of *Corynebacterium glutamicum* for production of amino acid L-alanine under oxygen deprivation. *Appl Microbiol Biotechnol* 87:159–165. <http://dx.doi.org/10.1007/s00253-010-2493-7>.
- Yamamoto S, Gunji W, Suzuki H, Toda H, Suda M, Jojima T, Inui M, Yukawa H. 2012. Overexpression of genes encoding glycolytic enzymes in *Corynebacterium glutamicum* enhances glucose metabolism and alanine production under oxygen deprivation conditions. *Appl Environ Microbiol* 78:4447–4457. <http://dx.doi.org/10.1128/AEM.07998-11>.
- Hasegawa S, Suda M, Uematsu K, Natsuma Y, Hiraga K, Jojima T, Inui M, Yukawa H. 2013. Engineering of *Corynebacterium glutamicum* for high-yield L-valine production under oxygen deprivation conditions. *Appl Environ Microbiol* 79:1250–1257. <http://dx.doi.org/10.1128/AEM.02806-12>.
- Sambrook J, Fritsch EF, Maniatis T. 1989. *Molecular cloning: a laboratory manual*, 2nd ed. Cold Spring Harbor Laboratory Press, Cold Spring Harbor, NY.
- Yukawa H, Omumasaba CA, Nonaka H, Kos P, Okai N, Suzuki N, Suda M, Tsuge Y, Watanabe J, Ikeda Y, Vertès AA, Inui M. 2007. Comparative analysis of the *Corynebacterium glutamicum* group and complete genome sequence of strain R. *Microbiology* 153:1042–1058. <http://dx.doi.org/10.1099/mic.0.2006/003657-0>.
- Vertès AA, Inui M, Kobayashi M, Kurusu Y, Yukawa H. 1993. Presence of *mrr*- and *mcr*-like restriction systems in coryneform bacteria. *Res Microbiol* 144:181–185. [http://dx.doi.org/10.1016/0923-2508\(93\)90043-2](http://dx.doi.org/10.1016/0923-2508(93)90043-2).
- Sanger F, Nicklen S, Coulson A. 1977. DNA sequencing with chain-terminating inhibitors. *Proc Natl Acad Sci U S A* 74:5463–5467. <http://dx.doi.org/10.1073/pnas.74.12.5463>.
- Riley J, Butler R, Ogilvie D, Finniear R, Jenner D, Powell S, Anand R, Smith J, Markham A. 1990. A novel, rapid method for the isolation of terminal sequences from yeast artificial chromosome (YAC) clones. *Nucleic Acids Res* 18:2887–2890. <http://dx.doi.org/10.1093/nar/18.10.2887>.
- Arai K, Fukushima T, Tomiya M, Mitsuhashi S, Sasaki T, Toyooka T. 2008. Simultaneous determination of N-acetylaspartylglutamate and N-acetylaspartate in rat brain homogenate using high-performance liquid chromatography with pre-column fluorescence derivatization. *J Chromatogr B Analyt Technol Biomed Life Sci* 875:358–362. <http://dx.doi.org/10.1016/j.jchromb.2008.09.010>.
- Morioka H, Miki Y, Saito K, Tomoo K, Ishida T, Hasegawa T, Yamano A, Takada C, Miyamoto K, Tsujibo H. 2010. Crystallization and preliminary X-ray crystallographic analysis of BxA, an intracellular beta-D-xylosidase from *Streptomyces thermoviolaceus* OPC-520. *Acta Crystallogr Sect F Struct Biol Cryst Commun* 66:791–793. <http://dx.doi.org/10.1107/S1744309110013400>.
- Schlosser A, Kampers T, Schrempf H. 1997. The *Streptomyces* ATP-binding component MsiK assists in cellobiose and maltose transport. *J Bacteriol* 179:2092–2095.
- Schlosser A, Jantos J, Hackmann K, Schrempf H. 1999. Characterization of the binding protein-dependent cellobiose and cellotriose transport system of the cellulose degrader *Streptomyces reticuli*. *Appl Environ Microbiol* 65:2636–2643.
- Vandermarliere E, Bourgeois T, Winn MD, van Campenhout S, Volckaert G, Delcour J, Strelkov S, Rabijns A, Courtin C. 2009. Structural analysis of a glycoside hydrolase family 43 arabinoxylan arabinofuranohydrolase in complex with xylo-tetraose reveals a different binding mechanism compared with other members of the same family. *Biochem J* 418:39–47. <http://dx.doi.org/10.1042/BJ20081256>.
- Kim YA, Yoon KH. 2010. Characterization of a *Paenibacillus woosongensis*

- sis beta-xylosidase/alpha-arabinofuranosidase produced by recombinant *Escherichia coli*. *J Microbiol Biotechnol* 20:1711–1716.
27. Czjzek M, Bravman T, Henrissat B, Shoham Y. 2004. Crystallization and preliminary crystallographic analysis of a thermostable family 52 beta-D-xylosidase from *Geobacillus stearothermophilus* T-6. *Acta Crystallogr D Biol Crystallogr* 60:1461–1463. <http://dx.doi.org/10.1107/S0907444904013320>.
  28. Pinphanichakarn P, Tangsakul T, Thongnumwon T, Talawanich Y, Thamchaipenet A. 2004. Purification and characterization of beta-xylosidase from *Streptomyces* sp. CH7 and its gene sequence analysis. *World J Microbiol Biotechnol* 20:727–733. <http://dx.doi.org/10.1007/s11274-004-4513-1>.
  29. Shao W, Xue Y, Wu A, Kataeva I, Pei J, Wu H, Wiegel J. 2011. Characterization of a novel beta-xylosidase, XylC, from *Thermoanaerobacterium saccharolyticum* JW/SL-YS485. *Appl Environ Microbiol* 77:719–726. <http://dx.doi.org/10.1128/AEM.01511-10>.
  30. Ferreira M, Sá-Nogueira I. 2010. A multitask ATPase serving different ABC-type sugar importers in *Bacillus subtilis*. *J Bacteriol* 192:5312–5318. <http://dx.doi.org/10.1128/JB.00832-10>.
  31. Kawaguchi H, Vertes AA, Okino S, Inui M, Yukawa H. 2006. Engineering of a xylose metabolic pathway in *Corynebacterium glutamicum*. *Appl Environ Microbiol* 72:3418–3428. <http://dx.doi.org/10.1128/AEM.72.5.3418-3428.2006>.
  32. Kang MK, Lee J, Um Y, Lee TS, Bott M, Park SJ, Woo HM. 2014. Synthetic biology platform of CoryneBrick vectors for gene expression in *Corynebacterium glutamicum* and its application to xylose utilization. *Appl Microbiol Biotechnol* 98:5991–6002. <http://dx.doi.org/10.1007/s00253-014-5714-7>.
  33. Radek A, Krumbach K, Gatgens J, Wendisch VF, Wiechert W, Bott M, Noack S, Marienhagen J. 2014. Engineering of *Corynebacterium glutamicum* for minimized carbon loss during utilization of D-xylose containing substrates. *J Biotechnol* 192:156–160. <http://dx.doi.org/10.1016/j.jbiotec.2014.09.026>.
  34. Jojima T, Noburyu R, Sasaki M, Tajima T, Suda M, Yukawa H, Inui M. 2015. Metabolic engineering for improved production of ethanol by *Corynebacterium glutamicum*. *Appl Microbiol Biotechnol* 99:1165–1172. <http://dx.doi.org/10.1007/s00253-014-6223-4>.
  35. Wang C, Zhang H, Cai H, Zhou Z, Chen Y, Ouyang P. 2014. Succinic acid production from corn cob hydrolysates by genetically engineered *Corynebacterium glutamicum*. *Appl Biochem Biotechnol* 172:340–350. <http://dx.doi.org/10.1007/s12010-013-0539-x>.
  36. Buschke N, Becker J, Schafer R, Kiefer P, Biedendieck R, Wittmann C. 2013. Systems metabolic engineering of xylose-utilizing *Corynebacterium glutamicum* for production of 1,5-diaminopentane. *Biotechnol J* 8:557–570. <http://dx.doi.org/10.1002/biot.201200367>.
  37. Meiswinkel TM, Gopinath V, Lindner SN, Nampoothiri KM, Wendisch VF. 2013. Accelerated pentose utilization by *Corynebacterium glutamicum* for accelerated production of lysine, glutamate, ornithine and putrescine. *Microb Biotechnol* 6:131–140. <http://dx.doi.org/10.1111/1751-7915.12001>.
  38. Gopinath V, Meiswinkel TM, Wendisch VF, Nampoothiri KM. 2011. Amino acid production from rice straw and wheat bran hydrolysates by recombinant pentose-utilizing *Corynebacterium glutamicum*. *Appl Microbiol Biotechnol* 92:985–996. <http://dx.doi.org/10.1007/s00253-011-3478-x>.